PHYSICAL REVIEW C **83**, 012801(R) (2011)

Quantum Monte Carlo study of dilute neutron matter at finite temperatures

Gabriel Wlazłowski and Piotr Magierski
Faculty of Physics, Warsaw University of Technology, Ulica Koszykowa 75, PL-00-662 Warsaw, Poland
(Received 6 December 2009; revised manuscript received 7 December 2010; published 31 January 2011)

We report results of fully nonperturbative, path integral Monte Carlo calculations for dilute neutron matter. The neutron-neutron interaction in the s channel is parameterized by the scattering length and the effective range. We calculate the energy and the chemical potential as a function of temperature at density $\rho = 0.003\,\mathrm{fm}^{-3}$. The critical temperature T_c for the superfluid-normal phase transition is estimated from the finite size scaling of the condensate fraction. At low temperatures we extract the spectral weight function $A(\mathbf{p}, \omega)$ from the imaginary time propagator using the methods of maximum entropy and singular value decomposition. We determine the quasiparticle spectrum, which can be accurately parameterized by three parameters: an effective mass m^*, a mean-field potential U, and a gap Δ. Large values of Δ/T_c indicate that the system is not a BCS-type superfluid at low temperatures.

DOI: 10.1103/PhysRevC.83.012801 PACS number(s): 21.65.Cd, 02.70.Ss, 03.75.Ss, 26.60.Kp

Dilute neutron matter is one of the simplest many-body nuclear systems. At sufficiently small densities its properties originate from the two-body s-wave interaction only. It is known that neutron matter has a positive pressure at all densities (contrary to nuclear matter) that prevents fragmentation, and it becomes superfluid at low temperatures. From a theoretical point of view, pure and dilute neutron matter is a fascinating system, since at a certain density range it becomes a nearly universal Fermi gas. Such systems are presently of great interest as a result of extraordinary progress in the field of cold atoms which has taken place over the last few years and has in fact opened a new chapter in many-body physics (see [1] and references therein). By taking advantage of the Feshbach resonances, experimentalists can control the strength of the atom-atom interaction and achieve the so-called unitary regime. This corresponds to the situation where the average distance between fermionic atoms is large compared to the interaction range r_0, but much smaller than the scattering length a, i.e., $\rho r_0^3 \ll 1 \ll \rho|a|^3$, where ρ is the particle number density. In the unitary regime the properties of dilute Fermi gases are universal, independent of the details of the interaction. The universality of these systems makes them a fascinating theoretical playground, and the results obtained turn out to be relevant to a wide range of fields such as string theory, the quark-gluon plasma, and high-T_c superconductors.

Since the $^1S_0$ neutron-neutron interaction is characterized by a large scattering length $a \approx -18.5\,\mathrm{fm}$, the unitary regime can be thought of as a limiting case of dilute neutron matter at a density range varying from 0.001 to $0.01\,\mathrm{fm}^{-3}$. One has to remember, however, that the influence of the effective range ($r_{\mathrm{eff}} \approx 2.8\,\mathrm{fm}$) cannot be ignored, since $k_F r_{\mathrm{eff}}$ is of the order of unity [2]. The importance of other channels, as well as of three-body forces, increases with density. However, at a density of $0.003\,\mathrm{fm}^{-3}$, which we study in this paper, their influence is marginal as compared to uncertainties regarding the path integral Monte Carlo (PIMC) method and therefore is neglected [3,4].

Since even for the density $\rho = 0.001\,\mathrm{fm}^{-3}$ dilute neutron matter is a strongly correlated Fermi gas ($|k_F a| \gg 1$), reliable insight into the physics of this system can be gained only by the use of nonperturbative approaches. Many such methods, known under the general name quantum Monte Carlo (QMC), have been used to date, although most of them concern zero temperature properties [5–7]. Finite temperature behavior has been studied in [8]. This work presents the first *ab initio*, fully nonperturbative evaluation of thermal properties of low-density neutron matter (at about 2% of nuclear saturation density) free of uncontrolled approximations within the PIMC method. We focus on the effects generated by the finite effective range.

Contrary to cold atomic gases, in order to capture the physics of dilute neutron matter one has to use more realistic interaction than a simple contact, deltalike force. In the present paper we employ two-body potential of the form

$$V(\mathbf{r}-\mathbf{r}') = \begin{cases} 6g, & \mathbf{r}-\mathbf{r}' = 0 \\ g, & \mathbf{r}-\mathbf{r}' \in \mathcal{N}_b \\ 0, & \text{otherwise} \end{cases}, \tag{1}$$

where $\mathcal{N}_b = \{(\pm b, 0, 0), (0, \pm b, 0), (0, 0, \pm b)\}$ represents the set of the nearest-neighbor coordinates. This particular form of the interaction is especially designed for the cubic lattice with lattice constant b and enables construction of a fully nonperturbative approach without the sign problem (for more details see Ref. [9]). It depends on two parameters (g and b) that are adjusted to correctly reproduce the scattering length and the effective range of neutron-neutron $^1S_0$ scattering amplitude [10]. Hence we consider the system on a three-dimensional spatial cubic lattice of length $L = N_s b$ with periodic boundary conditions. The lattice spacing b and size L introduce the natural ultraviolet (UV) and infrared momentum cutoffs given by $p_{\mathrm{cut}} = \pi/b$ and $p_0 = 2\pi/L$, respectively. The momentum space has the shape of a cubic lattice, with size $2\pi/b$ and spacing $2\pi/L$. To simplify the analysis, however, we place the spherically symmetric UV cutoff, including momenta $p \leqslant p_{\mathrm{cut}}$.

To numerically evaluate the expectation values of observables, we have followed the path integral approach described in Ref. [11]. Using Trotter expansion and subsequently

Hubbard-Stratonovich (H-S) transformation, evaluation of the emerging path integral was performed using the Metropolis importance sampling. The crucial modification of the procedure described in [11] consists of construction of the H-S transformation, which allows the off-site part of the interaction to be incorporated without generation of the sign problem. Specifically, we have used the discrete H-S transformation of the form [9]

$$e^{-\tau\hat{V}} = \prod_{\mathbf{r}-\mathbf{r}'\in\mathcal{N}_b}\prod_{\lambda=\uparrow\downarrow}\frac{1}{k}\sum_{i=1}^{k} e^{\sigma_i(\mathbf{r},\mathbf{r}')[\hat{n}_\lambda(\mathbf{r})+\hat{n}_\lambda(\mathbf{r}')]}, \qquad (2)$$

where σ_i are real numbers and $\hat{n}_\lambda(\mathbf{r})$ is the occupation number operator. The notable feature of this H-S transformation is the time reversal invariance of the corresponding imaginary time evolution operator. This property ensures that the probability measure used in the Metropolis algorithm is always positive [9,12].

Calculations were performed on a lattice of size $N_s = 8$, with the lattice constant $b = 3.21$ fm. The chemical potential was chosen in such a way to keep the total number of particles between 53 and 57, which corresponds to the density $k_F \simeq 0.45\,\mathrm{fm}^{-1}$. The temperatures span the interval from $0.06\,\varepsilon_F$ (0.26 MeV) to $1.0\,\varepsilon_F$ (4.3 MeV), where ε_F is the Fermi energy. The number of imaginary time steps required to reach the convergence of the algorithm varies with temperature. At the lowest temperature 2360 imaginary time steps have been applied, whereas for the highest temperature only 216. The kinetic energy part of the Hamiltonian is defined in the restricted momentum space ($p \leqslant p_{\mathrm{cut}}$) using the dispersion relation of the form $\varepsilon(\mathbf{p}) = p^2/2m$. Consequently, during the imaginary time evolution the fast Fourier transform (FFT) algorithm was used to switch between momentum and coordinate spaces [11]. The number of generated uncorrelated Monte Carlo samples allows the statistical error to decrease below 5%. At low temperatures the singular value decomposition technique was applied to avoid instabilities of the algorithm. In all runs the single-particle occupation probabilities for the highest energy states were below 1% at all temperatures. We have also performed a few exploratory simulations for the lattice of size $N_s = 10$. The results were in a good agreement with those for the $N_s = 8$ lattice.

In Fig. 1 the low-temperature behavior of the total energy and chemical potential is presented for two different lattice sizes. The (shifted) total energy versus temperature for the free Fermi gas (FFG) at the same particle density has also been plotted (solid line). Note that after shifting of the free Fermi gas energy by $0.52\,E_{\mathrm{FFG}}$ the curve reproduces Monte Carlo results for $T > 0.15\,\varepsilon_F$ ($E_{\mathrm{FFG}} = \frac{3}{5}N\varepsilon_F$ is the free Fermi gas energy at $T = 0$). Below this temperature the deviation from the free Fermi gas behavior is clearly visible. The chemical potential is approximately constant for $T < 0.1\,\varepsilon_F$.

The critical temperature of the superfluid-normal phase transition has been determined using a method based on the finite size scaling of the correlation function. A similar technique was used to determine the critical temperature at the unitary limit (see Refs. [11,13] for details). The volume-dependent estimation of the critical temperature $T_c^{(ij)}$ was obtained by finding the crossing point of the rescaled

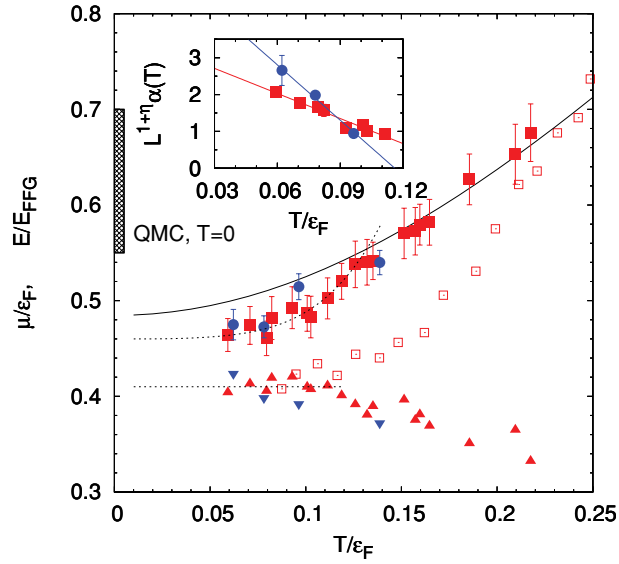

FIG. 1. (Color online) Total energy E and chemical potential μ as a function of temperature for dilute neutron matter at density $\rho = 0.003\,\mathrm{fm}^{-3}$ ($k_F \simeq 0.45\,\mathrm{fm}^{-1}$). The total energy is denoted by red squares (8^3 lattice) and blue circles (10^3 lattice). The red up triangles and blue down triangles correspond to the chemical potential for the 8^3 and 10^3 lattice, respectively. The solid line represents the energy of the noninteracting Fermi gas, shifted by a constant value. The dashed line shows an extrapolation of the energy and the chemical potential to $T = 0$ limit. For comparison the total energy of the unitary Fermi gas is also plotted (open red squares). The dashed area for $T = 0$ denotes the range where the results of other QMC results are located (see, for example, Ref. [6]). In the inset the rescaled condensate fraction is shown as a function of temperature, and red squares and blue circles denote 8^3 and 10^3 lattices, respectively. The crosspoint determines the critical temperature of the superfluid-normal phase transition, $T_c \approx 0.09\,\varepsilon_F$.

condensate fraction for two different lattice sizes $N_{i,j}$. As $N_{i,j} \to \infty$, the series $T_c^{(ij)}$ converges to T_c and one can extract the limiting value. We have determined T_c using results for two lattices, $N_{i,j} = 8, 10$. Such large lattices and rather small filling factors, which in both cases reads $\nu = N/2N_s^3 \approx 5\%$, are enough to estimate the critical temperature with uncertainty smaller than 20%. (In fact, this procedure applied to the unitary gas gives estimation of T_c with a relative error of less than than 10%.) The estimate of the critical temperature reads $T_c \approx 0.09\,\varepsilon_F$. Note that T_c is considerably lower than the temperature for the onset of deviation from the free Fermi gas behavior.

Within the PIMC framework one cannot directly reach the $T = 0$ limit. However, the ground-state energy can be obtained by performing an extrapolation of results to zero temperature limit. In our case this procedure provides the ground-state energy $E/E_{\mathrm{FFG}} = 0.46(2)$ [$E/N = 1.22(5)$ MeV]. This value is considerably lower (by about 20%–40%) than values obtained by other MC calculations (see, for example, Ref. [6]). This is most likely because our approach is based on fully unrestricted path integral calculations and, within statistical errors due to the Monte Carlo procedure, gives essentially exact results.

The gap in the fermionic spectrum, related to superfluidity, has been computed from the spectral weight function $A(\mathbf{p}, \omega)$ by performing the analytic continuation of the imaginary time propagator $\mathcal{G}(\mathbf{p}, \tau)$ to real frequencies [14]. This procedure is equivalent to solving the integral equation

$$\mathcal{G}(\mathbf{p}, \tau) = -\frac{1}{2\pi} \int_{-\infty}^{+\infty} d\omega A(\mathbf{p}, \omega) \frac{\exp(-\omega\tau)}{1 + \exp(-\omega\beta)}, \qquad (3)$$

where $\mathcal{G}(\mathbf{p}, \tau)$ is known from the Monte Carlo calculations for 51 different values of $\tau \in [0, \beta = 1/T]$. The inverse problem is, however, numerically ill-posed, i.e., there is an infinite class of solutions for $A(\mathbf{p}, \omega)$ which satisfy Eq. (3) within uncertainties generated by the Monte Carlo method. Therefore we have used two independent methods based on completely different mathematical approaches.

The first one, the maximum entropy method, is based on Bayes' theorem [15]. It treats the values of $\tilde{\mathcal{G}}(\mathbf{p}, \tau_i)$ $(i = 0, 1, \ldots, 50)$ provided by QMC simulation as normally distributed random numbers, around the true values $\mathcal{G}(\mathbf{p}, \tau_i)$, and searches for the most probable solution assuming some *a priori* knowledge concerning the spectral function. As *a priori* information we have used the following constraints:

$$A(\mathbf{p}, \omega) \geqslant 0, \quad \int_{-\infty}^{+\infty} \frac{d\omega}{2\pi} A(\mathbf{p}, \omega) = 1, \qquad (4)$$

$$\int_{-\infty}^{+\infty} \frac{d\omega}{2\pi} A(\mathbf{p}, \omega) \frac{1}{1 + \exp(\omega\beta)} = n(\mathbf{p}), \qquad (5)$$

and we have assumed a Gaussian-like structure for $A(\mathbf{p}, \omega)$. In the formula (5) $n(\mathbf{p})$ represents the occupation probability of the state with momentum $\mathbf{p}$ that is known from the Monte Carlo simulation.

The second method is based on the singular value decomposition (SVD) of the integral kernel $\mathcal{K}$ of Eq. (3), which can be rewritten in operator form as $\mathcal{G}(\mathbf{p}, \tau_i) = (\mathcal{K}A)(\mathbf{p}, \tau_i)$. The operator $\mathcal{K}$ possesses the singular system, which forms a suitable basis for the expansion of the projected spectral weight function $\tilde{A}(\mathbf{p}, \omega)$ onto a subspace where the inverse problem is well-posed [16]. Since the method provides only a projection of the "true" solution, it does not require any *a priori* information, contrary to the maximum entropy method. However, since $\mathcal{G}(\mathbf{p}, \tau_i)$ includes statistical errors due to the Monte Carlo procedure, the projected solution $\tilde{A}(\mathbf{p}, \omega)$ is also affected by this uncertainty. One can use this flexibility by choosing the solution satisfying the constraints (4) [17]. The details of both methods will be discussed elsewhere [18].

The spectral weight function for the lowest temperature $T = 0.06\,\varepsilon_F$ obtained for an $N_s = 10$ lattice is shown in the Fig. 2. The same outcome has been generated by both methods (maximum entropy and SVD) independently. The presence of a "pairing" gap is clearly visible for this temperature.

Figure 3 presents the quasiparticle excitation spectrum extracted from the spectral weight function for $T = 0.06\,\varepsilon_F$. We have found that the quasiparticle excitations can be accurately parameterized by the BCS-like formula,

$$E(\mathbf{p}) = \pm\sqrt{\left(\frac{\mathbf{p}^2}{2m^*} - \mu + U\right)^2 + \Delta^2}, \qquad (6)$$

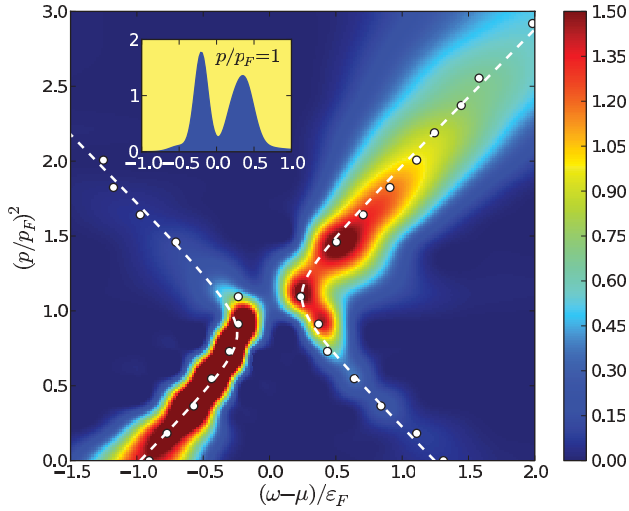

FIG. 2. (Color online) Spectral weight function $A(\mathbf{p}, \omega)$ at the temperature $T = 0.06\,\varepsilon_F$ and lattice size $N_s = 10$ obtained by the maximum entropy method. Points indicate localizations of maxima for fixed values of momenta. Dashed lines correspond to the fit of the BCS-type formula given by (6). In the inset the spectral weight function at the Fermi level is presented.

where m^* is an effective mass, U the mean field potential, and Δ is the "pairing" gap. The values of these parameters were estimated as $m^*/m = 1.1(1)$, $U/\varepsilon_F = -0.26(6)$, and $\Delta/\varepsilon_F = 0.25(5)$.

Note that the ratio $\Delta/T_c \approx 2.8$ is significantly higher than the well-known value 1.76 predicted by BCS theory. The similar deviation from the BCS value is typical for high-temperature superconductors [19] and also for cold atomic gases in the unitary regime [11]. Therefore we conclude that the dilute neutron matter at this density is not a BCS-type superfluid. Note also that to estimate the value of Δ/T_c we have used the value of the energy gap at the temperature

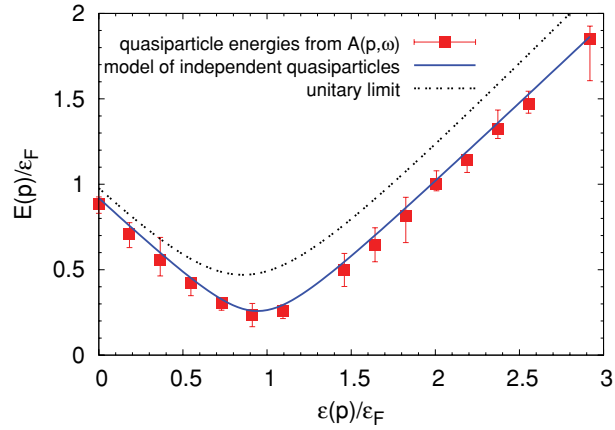

FIG. 3. (Color online) Quasiparticle energies $E(\mathbf{p})$ (squares) extracted from the spectral weight function $A(\mathbf{p}, \omega)$ at $T = 0.06\,\varepsilon_F$. The line denotes results obtained under the assumption that the system is composed of independent quasiparticles. The dashed line corresponds to quasiparticle energies at the unitary limit.

$T = 0.06\,\varepsilon_F$, which is expected to be slightly lower than the value of the gap at zero temperature.

It is instructive to compare quasiparticle excitation energies with those extracted from the susceptibility function under the assumption that the system is composed of independent quasiparticles. Under this assumption the imaginary time propagator is simply given by

$$\mathcal{G}(\mathbf{p},\tau) = -\frac{e^{-\tau E(\mathbf{p})}}{1+e^{-\beta E(\mathbf{p})}}, \tag{7}$$

and one can easily evaluate the susceptibility

$$\chi(\mathbf{p}) = -\int_0^\beta d\tau\, \mathcal{G}(\mathbf{p},\tau) = \frac{1}{E(\mathbf{p})}\frac{e^{\beta E(\mathbf{p})}-1}{e^{\beta E(\mathbf{p})}+1}. \tag{8}$$

From the calculated one-body propagator within the Monte Carlo algorithm one can extract the spectrum of the elementary fermionic excitations by inverting Eq. (8). The extracted spectrum of quasiparticle energies turns out to reproduce very well (within error bars) the quasiparticle spectrum derived from the spectral function (see Fig. 3). The same property is shared by unitary cold atomic gas at temperatures below the critical temperature [20].

Comparison of our results with those obtained in the limit $r_{\text{eff}} \to 0$ provides information about the influence of the effective range. From the data reported in Ref. [11] we infer that the effects of the effective range do not significantly alter the ground-state energy. The value of the energy gap and the critical temperature decreases considerably (at $r_{\text{eff}} \to 0$: $\Delta^{(0)}/\varepsilon_F \approx 0.41$ and $T_c^{(0)}/\varepsilon_F \approx 0.13$). However, surprisingly the ratio $\Delta^{(0)}/T_c^{(0)} \approx 3.2$ remains approximately constant (taking into account the uncertainties of our estimation) when increasing r_{eff} to the value associated with $^1S_0$ neutron-neutron interaction. Note also that the equation of state exhibits the existence of the second temperature scale, which can be attributed to the onset of deviations of E/E_{FFG} from the (shifted) energy of the free Fermi gas. It bears similarity to the case of the unitary Fermi gas, where the existence of the so-called "pseudogap" above T_c is reported [20].

Summarizing, our results do not indicate the presence of qualitative changes in comparison to the case of zero effective range. In conclusion, the main aspects of physics at the unitary regime survive within the limit of dilute neutron matter.

We thank Aurel Bulgac for discussions. Support from the Polish Ministry of Science under Contracts No. N N202 328234 and No. N N202 128439, and from the UNEDF SciDAC Collaboration under DOE grant DE-FC02-07ER41457 is gratefully acknowledged. Use of computers at the Interdisciplinary Centre for Mathematical and Computational Modelling (ICM) at Warsaw University is also gratefully acknowledged.

[1] S. Giorgini, L. P. Pitaevskii, and S. Stringari, Rev. Mod. Phys. **80**, 1215 (2008); I. Bloch, J. Dalibard, and W. Zwerger, Rev. Mod. Phys. **80**, 885 (2008).

[2] A. Schwenk and C. J. Pethick, Phys. Rev. Lett. **95**, 160401 (2005).

[3] M. Baldo and C. Maieron, Phys. Rev. C **77**, 015801 (2008).

[4] A. Gezerlis and J. Carlson, Phys. Rev. C **81**, 025803 (2010).

[5] S. Fantoni, A. Sarsa, and K. E. Schmidt, Phys. Rev. Lett. **87**, 181101 (2001); J. Morales, V. R. Pandharipande, and D. G. Ravenhall, Phys. Rev. C **66**, 054308 (2002); L. Brualla, S. Fantoni, A. Sarsa, K. E. Schmidt, and S. A. Vitiello, *ibid.* **67**, 065806 (2003); A. Sarsa, S. Fantoni, K. E. Schmidt, and F. Pederiva, *ibid.* **68**, 024308 (2003); J. Carlson, J. Morales, V. R. Pandharipande, and D. G. Ravenhall, *ibid.* **68**, 025802 (2003); S. Y. Chang *et al.*, Nucl. Phys. A **746**, 215 (2004); A. Fabrocini, S. Fantoni, A. Y. Illarionov, and K. E. Schmidt, Phys. Rev. Lett. **95**, 192501 (2005); A. Gezerlis and J. Carlson, Phys. Rev. C **77**, 032801(R) (2008).

[6] S. Gandolfi, A. Y. Illarionov, S. Fantoni, F. Pederiva, and K. E. Schmidt, Phys. Rev. Lett. **101**, 132501 (2008); S. Gandolf, A. Y. Illarionov, S. Fantoni, K. E. Schmidt, F. Pederiva, and S. Fantoni, Phys. Rev. C **79**, 054005 (2009); S. Gandolfi, A. Y. Illarionov, F. Pederiva, K. E. Schmidt, and S. Fantoni, *ibid.* **80**, 045802 (2009).

[7] E. Epelbaum *et al.*, Eur. Phys. J. A **40**, 199 (2009).

[8] H.-M. Muller, S. E. Koonin, R. Seki, and U. vanKolck, Phys. Rev. C **61**, 044320 (2000); D. Lee, B. Borasoy, and T. Schaefer, *ibid.* **70**, 014007 (2004); D. Lee and T. Schäfer, *ibid.* **72**, 024006 (2005); **73**, 015201 (2006); **73**, 015202 (2006); T. Abe and R. Seki, *ibid.* **79**, 054002 (2009).

[9] G. Wlazłowski and P. Magierski, Int. J. Mod. Phys. E **18**, 919 (2009).

[10] G. Wlazłowski and P. Magierski, Int. J. Mod. Phys. E **19**, 781 (2010).

[11] A. Bulgac, J. E. Drut, and P. Magierski, Phys. Rev. A **78**, 023625 (2008).

[12] S. E. Koonin, D. J. Dean, and K. Langanke, Phys. Rep. **278**, 1 (1997).

[13] E. Burovski, N. Prokofev, B. Svistunov, and M. Troyer, Phys. Rev. Lett. **96**, 160402 (2006).

[14] A. A. Abrikosov *et al.*, *Methods of Quantum Field Theory in Statistical Physics* (Dover, New York, 1975); A. L. Fetter and J. D. Walecka, *Quantum Theory of Many-Particle Systems*, (Dover, New York, 2003).

[15] E. T. Jaynes, in *The Maximum Entropy Formalism*, edited by R. D. Levine and M. Tribus (MIT Press, Cambridge, 1978), pp. 15–118; R. N. Silver, D. S. Sivia, and J. E. Gubernatis, Phys. Rev. B **41**, 2380 (1990); R. N. Silver, J. E. Gubernatis, D. S. Sivia, and M. Jarrell, Phys. Rev. Lett. **65**, 496 (1990); S. R. White, Phys. Rev. B **44**, 4670 (1991).

[16] M. Bertero, C. de Mol, and E. R. Pike, Inverse Probl. **1**, 301 (1985); **4**, 573 (1988); C. E. Creffield, E. G. Klepfish, E. R. Pike, and S. Sarkar, Phys. Rev. Lett. **75**, 517 (1995).

[17] G. D. de Villiers, B. McNally, and E. R. Pike, Inverse Probl. **15**, 615 (1999).

[18] P. Magierski and G. Wlazłowski (in preparation).

[19] Ø. Fischer, M. Kugler, I. Maggio-Aprile, C. Berthod, and C. Renner, Rev. Mod. Phys. **79**, 353 (2007).

[20] P. Magierski, G. Wlazłowski, A. Bulgac, and J. E. Drut, Phys. Rev. Lett. **103**, 210403 (2009).